Equivalent Model of Photoswitch: Application to the UWB Antenna Design Integrating Impulse Feeding

Valerie Bertrand[1, *], Romain Négrier[2], Michele Lalande[2], Joel Andrieu[2], Vincent Couderc[3], Badr M. Shalaby[4], Laurent Pecastaing[5], and Antoine De Ferron[5]

Abstract—Optoelectronic devices triggered by a laser flash and operating in linear switching regime allow the generation of short pulses with small time jitters (2 ps typically). An Ultra Wide Band antenna array combining as many of this photoswitches as antennas has the advantage to increase the radiation power on one hand and to offer the agility of the radiation beam on the other hand obtained by time delay of laser illumination. During the step of antenna design, it becomes important to take into account the photoswitch integration in order to increase the peak power and the frequency band of the generated output signal. This paper presents an equivalent model of photoswitch obtained with the transient solver of CST Microwave Studio coupled within CST Design Studio. The second part of this article is dedicated to the integration of a photoswitch even within the antenna.

1. INTRODUCTION

The radiated waveform generation via optoelectronic devices presents many interests for the possibility of beamforming via optical delay and the limitation of coaxial connection problems [1–3]. Previous studies performed by XLIM and CISTEME demonstrated the feasibility of a system combining "*n*" optoelectronic sources to "*n*" antennas triggered by a laser flash. The electric field radiated by each elementary source is added in a direction which depends on the time of illumination of photoswitches, with a jitter lower than 2 ps. The applications developed on this principle are UWB synthetic aperture radar (SAR) [4] and high power UWB radiation source [5].

The modular aspect of these demonstrators had been kept by associating photoswitch with the antenna via coaxial connectors and cables. The use of these components can limit the peak voltage level accepted by the antenna and the frequency band. In order to overcome this limitation, it seems interesting to integrate the photoswitch into the antenna in freeing itself from any coaxial connectors [6].

The type of photoswitch usually used in our devices operates in the linear regime and is comparable to voltage controlled switch. The behavior of the latter can be taken into account in simulation through coupling between a method of electromagnetic simulation and one of electrical circuit simulation. In this case, it is co-simulation between CST Microwave Studio (MWS) and CST Design Studio (DS). Indeed, the transient 3D EM/circuit co-simulation is suitable for many application areas as antenna design [7], filter tuning, UWB applications, etc. [8]. The first part of this article presents the simulation of the behavior of a photoswitch in coplanar technology and the validation of the model. In the second section, a microstrip photoswitch is integrated into an antenna developed in previous works.
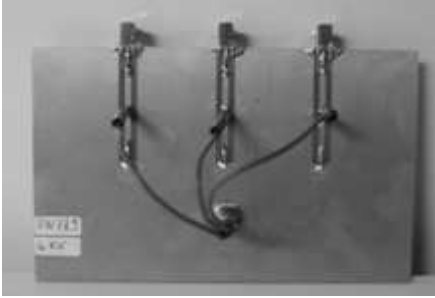
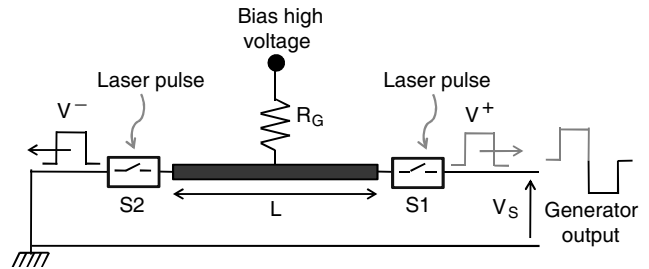**Figure 1.** Three photoswitches in coplanar waveguide technology.

Figure 2. Bipolar frozen-wave generator principle.

2. PHOTOSWITCH

2.1. Optical Bipolar Pulses Generator

Photoswitches taken as example in this paper (Figure 1) were developed in coplanar waveguide technology to feed a 4×3 UWB antenna array [4]. These optical generators can generate electrical bipolar short pulses by using the well-known "frozen wave generator" [9–12]. The interest of the bipolar pulses is that they improve the radiation efficiency of UWB antennas.

The generator consists in a $50\,\Omega$ impedance coplanar transmission waveguide. At one end, the line is connected to a $50\,\Omega$ load or an UWB antenna via a photoconductive switch $S1$ (Figure 2). The other end is short-circuited via a second switch $S2$. Photoconductors are specific silicon diodes and are able to support high voltage. During the off-state, the line is fully charged and opened at both ends. When photoswitches close simultaneously via laser pulses, a bipolar electric pulse is generated to the $50\,\Omega$ load. The bipolar pulse duration is directly dependent of the charged line length. In this case, the storage line length is $38\,\text{mm}$. The bias voltage used to polarize the switches is set less than $2\,\text{kV}$. This two switches are activated by means of a flash-pumped Nd: YAG laser delivering picoseconds pulses with $25\,\text{ps}$ duration at $1064\,\text{nm}$ at a $20\,\text{Hz}$ pulse repetition frequency.

By illuminating the two photoconductive devices with two optical signals without delay, an electrical bipolar pulse is generated with duration of $650\,\text{ps}$ and a bandwidth of $2.7\,\text{GHz}$ at $-10\,\text{dB}$ (Figure 3).
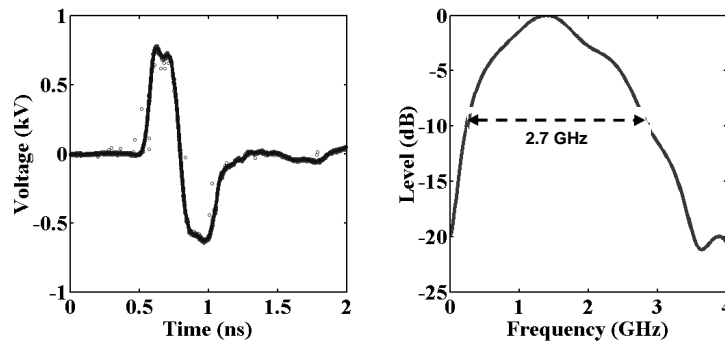

Figure 3. Bipolar pulse of $650\,\text{ps}$ and its normalized spectrum.

2.2. Photoswitch Model with CST Studio Suite

Previous photoconductors operating in linear regime can be modeled as voltage controlled switches. The photoswitch behavior is modeled by coupling simulation between CST MWS and CST DS. CST MWS allows modeling the propagation line and later the line-antenna system. The model created under CST
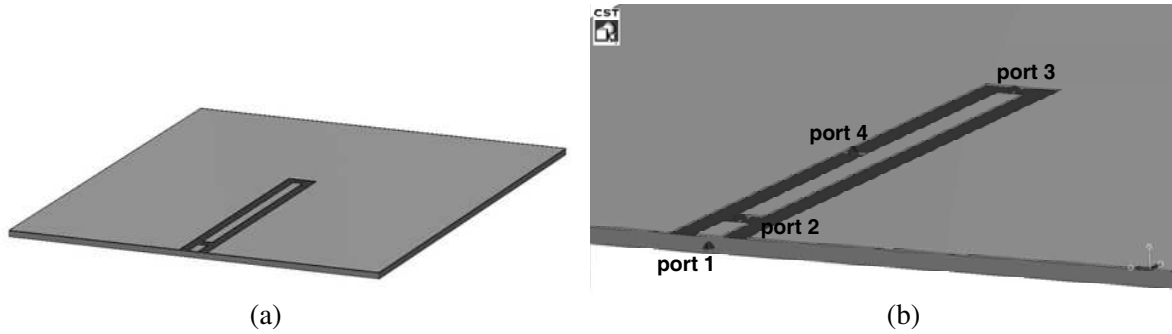
Figure 4. 3D view of coplanar waveguide for EM simulation with CST MWS. (a) General view. (b) Zoom on coplanar waveguide with port location.
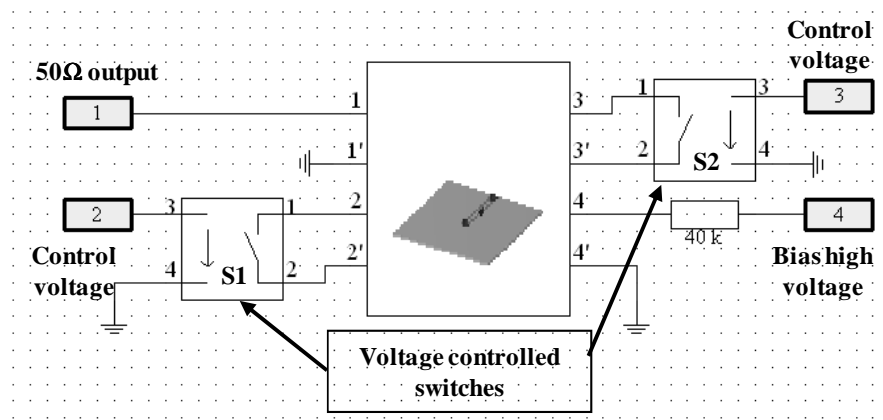

Figure 5. Circuit model of the photoswitch.

MWS takes into account geometrical characteristics of coplanar waveguide and dielectric characteristics of epoxy substrate (Figure 4). Thereafter, adding ports in the 3D model creates input-output access between the two simulation tools.

The 3D model is represented as a block diagram in CST DS. Generators and circuits are added and connected to the different ports numbered 1 to 4 (Figure 5). External ports are defined as follows: external port 1 is a $50\,\Omega$ output (generated signal), external ports 2 and 3 are the voltage controlled switches and external port 4 is the polarization high-voltage of $2\,\text{kV}$ level. A $40\,\text{k}\Omega$ resistor is added in series with the external port 4 to take into account the internal resistance of the high voltage generator. The equivalent resistance of the switch is $300\,\text{M}\Omega$ at off-state and $3\,\Omega$ at on-state which is compliance with the practice. The control voltage is a square pulse of $1\,\text{V}$ peak level. Switches are triggered for $t = 1390\,\text{ns}$ when the line is loaded.

The first graph of Figure 6 shows the charging voltage of the coplanar transmission line. The switches are closed at $t = 1390\,\text{ns}$. After the closing of switches, we can observe the discharge line and the generation of the short pulse.

The generated voltage is a bipolar form in accordance with the principle of frozen wave generator (Figure 7). The experimental and theoretical voltages are similar: transient shapes, duration around $700\,\text{ps}$ and bandwidth of $2.6\,\text{GHz}$ at $-10\,\text{dB}$. The theoretical efficiency is perfect unlike experimentation which can explain the differences in peak levels. In conclusion, this theoretical approach is suitable for antenna design with integrated photoswitch.

3. INTEGRATION INTO ANTENNA

The considered UWB antenna is inspired by the antenna developed by Koshelev et al. [13]. This antenna combines the radiation mode of a traveling wave antenna with that of a magnetic loop. Figure 8 presents
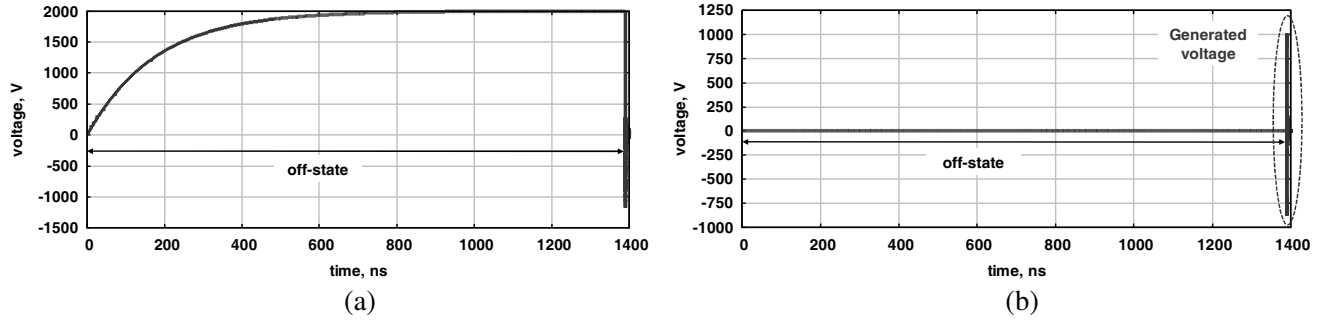
Figure 6. Charging voltage of (a) the coplanar waveguide and (b) generated voltage.
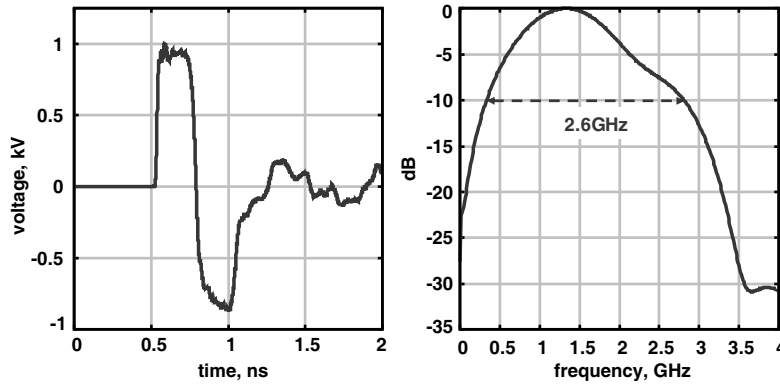

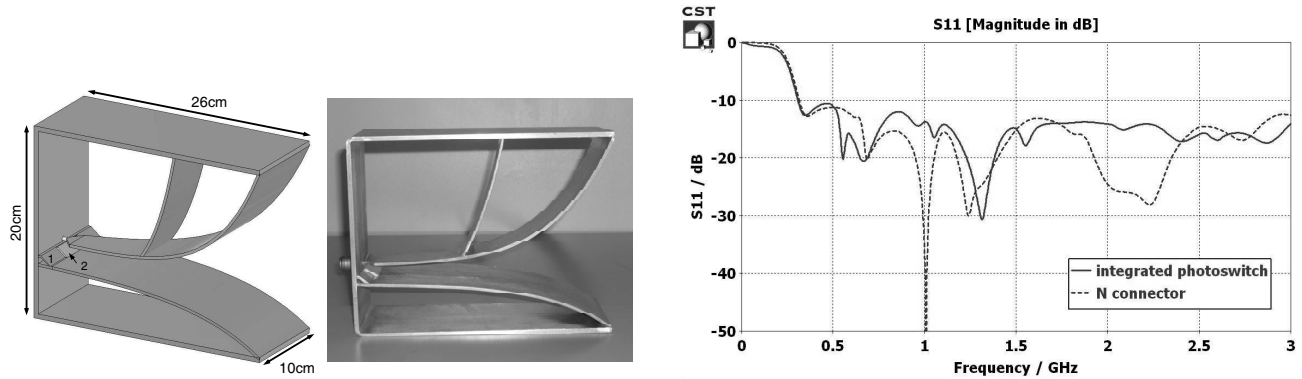**Figure 7.** Theoretical bipolar pulse and its normalized spectrum.

Figure 8. The UWB antenna (CAD model and realized geometry).

Figure 9. Reflection coefficient.

the antenna and its adequate transition: piece 1 is made of metal while piece 2 is made of PTFE and permits a high voltage application. The main dimensions of antenna shown Figure 8 are: 26 cm in length, 20 cm in height, 10 cm in width. The supply connector is a coaxial connector N. This antenna has been designed with the CST MWS software and can support a transient voltage of 10 kV. The matching bandwidth at -10 dB is between 300 MHz and 3 GHz (Figure 9).

The antenna input starts with a propagation structure similar to a microstrip line. It appears clear to insert the photoswitch with microstrip technology upstream of the flared part of the antenna (Figure 10). This means lengthening the antenna of five centimeters while keeping the same flare. In addition, to prevent inopportune breakdowns between the ground and line, it is better to implement
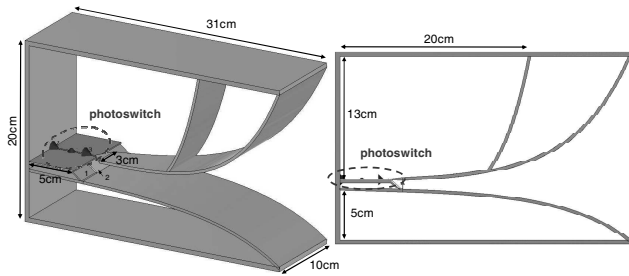
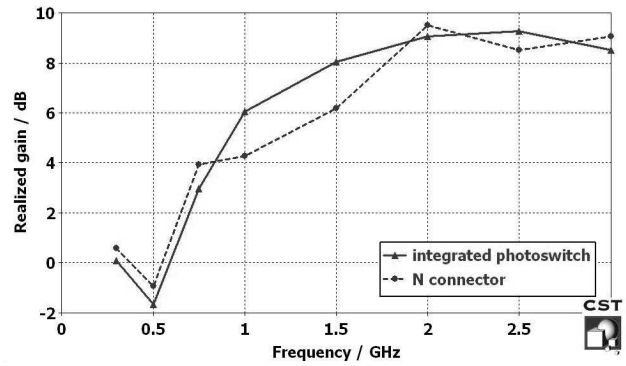**Figure 10.** Views of the antenna with integrated photoconductor device.

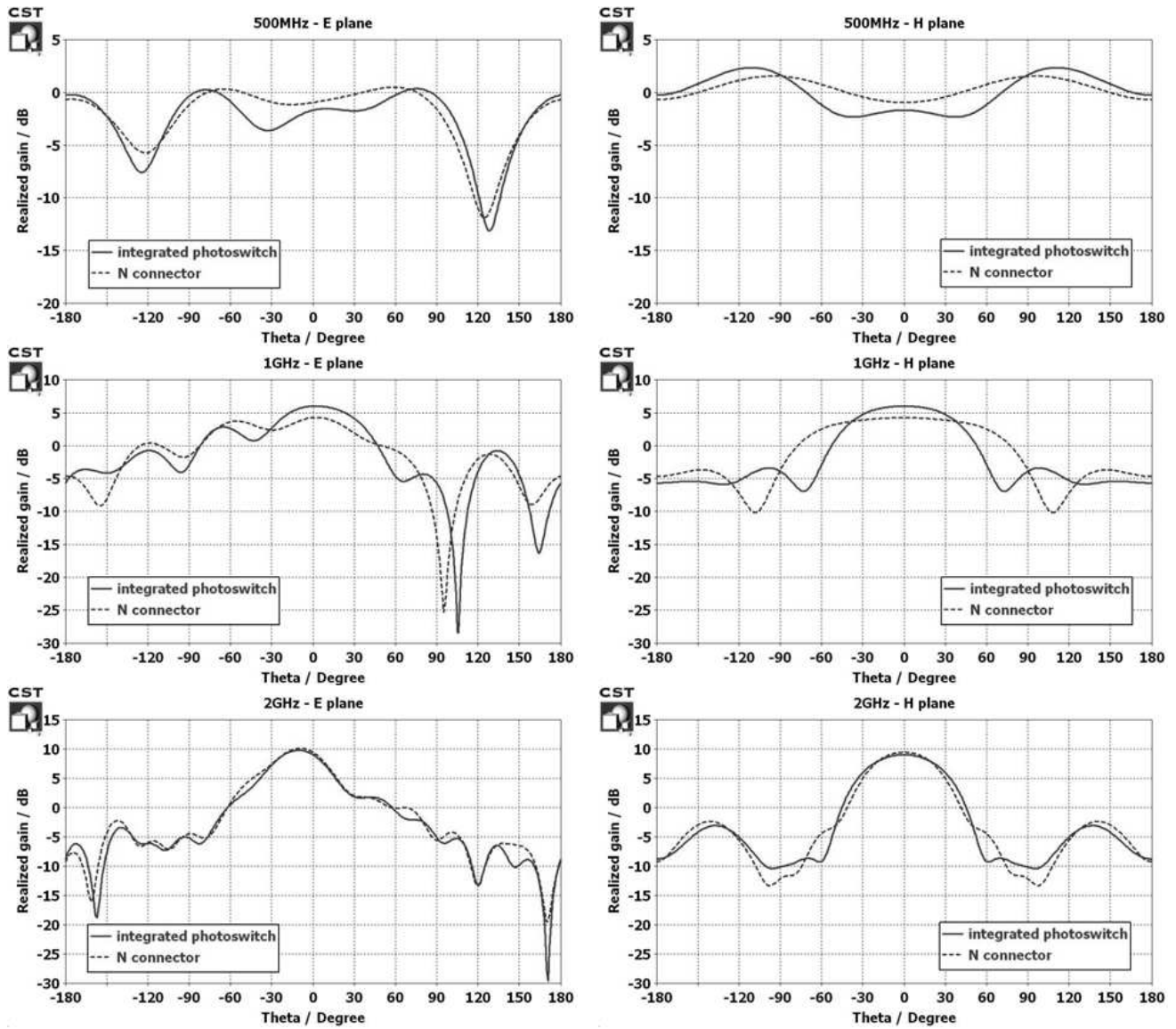**Figure 11.** Realized gain in the main radiation direction.

Figure 12. Radiation patterns for E and H planes.

the photoconductor on a microstrip line (the ground on one side and the line on the other side) rather than on a coplanar waveguide (ground plane and polarized line in the same plane). The integrated photoswitch consists of a $50\,\Omega$ microstrip line. The line length is $38\,\text{mm}$ like the previous photoswitch to generate a pulse of the same duration. The bias voltage is $12\,\text{kV}$, as this will be the case for future experiments. The matching bandwidth of the antenna with integrated photoswitch is identical to that of the original antenna (Figure 9).

The Figure 11 shows that the realized gain is small at low frequencies of adaptation bandwidth. The photoswitch integration allows greatly improve the gain at $1\,\text{GHz}$ and $1.5\,\text{GHz}$.

Radiation patterns of antennas in E and H planes are presented Figure 12. The extension of the antenna contributes to modify radiation patterns at the low part of the frequency bandwidth. Especially, we observe much more directive patterns at $1\,\text{GHz}$.

One of the advantages of the photoswitch integration in the antenna simulation is to get the corresponding transient shape of the radiated field which can be useful for the treatment of radar imaging for example. To illustrate this point, the radiation in the axis of the antenna with integrated photoswitch (Figure 10) is compared with that of the antenna (Figure 8) associated with an identical photoswitch via N coaxial connectors. The voltages calculated at the antenna input, i.e., at the beginning of the flare are shown Figure 13. The transient waveforms are equivalent but the signal level is lower in the case of system combining the antenna and the photoswitch via N connectors. This difference is explained by the presence of the discontinuity between the microstrip line of photoswitch and the N connector.

The same phenomena are observed on the electric fields radiated in the axis (amplitude of the radiated farfield reduced to the distance $r = 1\,\text{m}$: rEd): preserved transient waveforms, lower levels for associating the antenna and the photoswitch via N connectors (Figure 14). The peak to peak level difference of electric fields is about 14%.

The results presented in this paragraph show an improvement of radiation in the axis of the antenna. The integration of the photoswitch (no coaxial connector) and also the lengthening of the antenna contribute to this improvement.
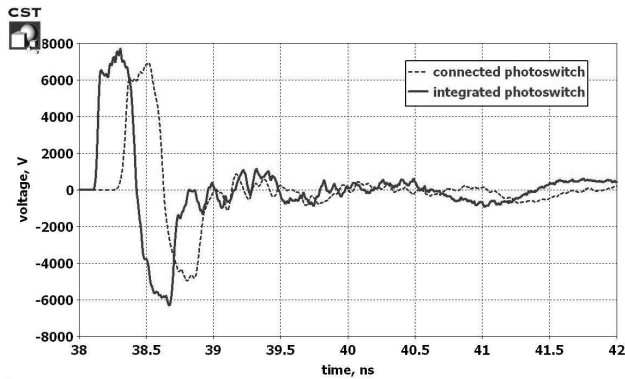

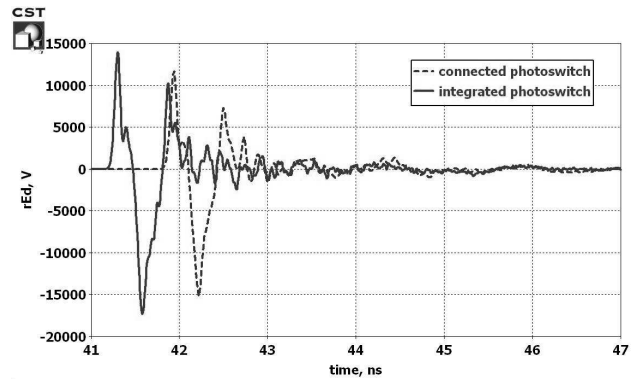**Figure 13.** Voltage waveform at the antenna input.

Figure 14. Waveforms of radiated electric fields.

4. CONCLUSION

It was shown the ability to model and simulate a generator whose behavior is similar to that of a photoswitch working in linear regime with coupled electromagnetic/circuit methods under CST Studio Suite. The theoretical signals generated on a coplanar waveguide are very close to the experimental ones. Simulations of the integration of a microstrip photoswitch into an existing antenna showed an improvement of the performance of the source/antenna system. The advantage of this approach will be more important for the future development of UWB radar and high power UWB radiation source with higher frequency bandwidth and/or higher voltage levels.

ACKNOWLEDGMENT

REFERENCES

1. Rotman, R., O. Raz, S. Barzilay, S. R. Rotman, and M. Tur, "Wideband antenna patterns and impulse response of broadband RF phased arrays with RF and photonic beamforming," *IEEE Transactions on Antennas and Propagation*, Vol. 55, No. 1, 36–44, Jan. 2007.

2. Bratchilov, A. N., "Photonic beamforming in ultra-wideband phased antenna arrays: Present state and perspectives," *Ultrawideband and Ultrashort Impulse Signals*, 159–164, Sevastopol, Ukraine, Sep. 18–22, 2006.

3. Lee, J. J., S. Livingston, B. Loo, V. Jones, and C. Foster, "Performance of an optically fed conformal array," *Antennas and Propagation Society International Symposium, 1994, AP-S Digest*, Vol. 2, 828–831, 1994, Digital Object Identifier: 10.1109/APS.1994.407964.

4. Godard, A., L. Desrumaux, V. Bertrand, J. Andrieu, M. Lalande, B. Jecko, M. Brishoual, V. Couderc, and R. Guillerey, "A transient UWB array used with complex impedance surfaces," *International Journal of Antennas and Propagation*, Vol. 2010, Article ID 243145, 8 Pages, 2010.

5. Desrumaux, L., A. Godard, M. Lalande, V. Bertrand, J. Andrieu, and B. Jecko, "An original antenna for transient high power UWB arrays: The shark antenna," *IEEE Transactions on Antennas and Propagation*, Vol. 58, No. 8, 2515–2522, 2010.

6. Chizh, A., S. Malyshev, S. Jefremov, B. Levitas, and I. Naidionova, "Impulse transmitting photonic antenna for ultra-wideband applications," *18th International Conference on Microwave Radar Wireless Communications (MIKON)*, 1–3, Vilnius, Lithuania, Jun. 14–16, 2010, ISBN 978-1-4244-5288-0.

7. Sotoudeh, O. and T. Wittig, "Electromagnetic simulation of mobile phone antenna performance," *Microwave Journal*, Jan. 2008.

8. Scott, A. and V. Sokol, "True transient 3D EM/circuit co-simulation using CST studio suite," *Microwave Product Digest*, 7–8, Oct. 2008.

9. Zu, L. Q., Y. Lu, H. Shen, and M. Dutta, "Temperature-dependent delay time in GaAs high-power high-speed photoconductive switching device," *IEEE Photonics Technology Letters*, Vol. 7, No. 1, 56–58, Jan. 1995.

10. Vergne, B., V. Couderc, A. Barthélémy, M. Lalande, V. Bertrand, and D. Gontier, "High-power bipolar picosecond pulse generation using optically activated traveling wave generator," *Microwave and Optical Technology Letters*, Vol. 48, No. 8, 1645–1648, Aug. 2008.

11. Amari, S. E., M. Kenaan, C. Merla, B. Vergne, D. Arnaud-Cormos, P. Leveque, and V. Couderc, "Kilovolt, nanosecond, and picosecond electric pulse shaping by using optoelectronic switching," *IEEE Photonics Technology Letters*, Vol. 22, No. 21, 1577–1579, Nov. 2010.

12. Merla, C., S. El. Amari, M. Kenaan, M. Liberti, F. Apollonio, D. Arnaud-Cormos, and V. Couderc, "A 10-Ω high-voltage nanosecond pulse generator," *IEEE Transactions on Microwave Theory and Techniques*, Vol. 58, No. 12, 4079–4085, Dec. 2010.

13. Koshelev, V. I., Y. I. Buyanov, Y. A. Andreev, V. V. Plisko, and K. N. Sukhushin, "Ultrawideband radiators of high-power pulses," *Pulsed Power Plasma Science 2001, Digest of Technical Papers*, Vol. 2, 1661–1664, Jun. 2001.